Innovative Food Science and Emerging Technologies 60 (2020) 102288

Contents lists available at ScienceDirect

Innovative Food Science and Emerging Technologies

journal homepage: www.elsevier.com/locate/ifset

High-voltage pulsed electric field laboratory device with asymmetric voltage multiplier for marine macroalgae electroporation

Klimentiy Levkov[a], Yoav Linzon[b], Borja Mercadal[c], Antoni Ivorra[c,d], César Antonio González[e], Alexander Golberg[a,*]

[a] Porter School of Environment and Earth Sciences, Tel Aviv University, Tel Aviv, Israel
[b] School of Mechanical Engineering, Tel Aviv University, Tel Aviv, Israel
[c] Department of Information and Communication Technologies, Universitat Pompeu Fabra, Barcelona, Spain
[d] Serra Húnter Fellow Programme, Universitat Pompeu Fabra, Barcelona, Spain
[e] Instituto Politécnico Nacional - Escuela Superior de Medicina, Mexico

ARTICLE INFO

Keywords:
Pulsed electric field generator
Electroporation
Biomass processing
Macroalgae
Bioimpedance
Bioeconomy

ABSTRACT

Optimization of protocols is required for each specific type of biomass processed by electroporation of the cell membrane with high voltage pulsed electric fields (PEF). Such optimization requires convenient and adaptable laboratory systems, which will enable determination of both electrical and mechanical parameters for successful electroporation and fractionation. In this work, we report on a laboratory PEF system consisting of a high voltage generator with a novel asymmetric voltage multiplying architecture and a treatment chamber with sliding electrodes. The system allows applying pulses of up to 4 kV and 1 kA with a pulse duration between 1 μs and 100 μs. The allowable energy dissipated per pulse on electroporated biomass is determined by the conditions for cooling the biomass in the electroporation cell. The device was tested on highly conductive green macroalgae from *Ulva* sp., a promising but challenging feedstock for the biorefinery. Successful electroporation was confirmed with bioimpedance measurements.

Industrial relevance: Seaweed biomass is an emerging feedstock for biorefineries with already 30 million tons per year of global industrial production. However, most of the biomass produced today is lost. Pulsed electric field (PEF) extraction could allow saving energy on biomass drying, deashing and it could allow extracting various organic compounds. However, the parameters needed to seaweed biomass treatment with PEF are not known and will differ from species to species. Furthermore, very high salt content challenges most of the available laboratory PEF devices, limiting the ability for parameters optimization in the lab. The developed laboratory scale PEF system coupled to bioimpedance measurement provides a necessary set of tools and methods for PEF parameters optimization required for process scale-up.

1. Introduction

Bioeconomy is the emerging sector of the economy which aims to develop sustainable biomass-based products for energy, food and chemical sectors (Bugge, Hansen, & Klitkou, 2016). One of the major technological challenges for bioeconomy is biomass fractionation, or biorefining: similar to oil or gas cracking or refining (Maity, 2015). An important step in those biomass fractionation processes is the breakdown of cell membranes (Günerken et al., 2015; Lee, Cho, Chang, & Oh, 2017). This breakdown allows for efficient separation of water from organic material (drying) and also it enables extraction for various useful intercellular components such as proteins, amino acids, lipids, carotenoids, and other molecules, each of which already has significant market value (Mussatto, 2016; Rinaldi, 2014). One type of these fractionation technologies is based on the use of high voltage, short-pulsed electric fields (PEFs) (Golberg et al., 2016).

Abbreviations: PEF, pulse electric field; CPE, constant phase element; ω, frequency (in rads/s); j, imaginary number; Z, impedance; R_∞, sample impedance at infinite frequency; R_0, sample impedance at zero frequency; τ, the characteristic time constant of the sample; α, a dimensionless parameter with a theoretical value between 0 and 1; Q_0, the capacitance value of the seaweed in the chamber; ESC, energy storage capacitor; EPC, electroporation cell; U_{ESC}, voltage on the storage capacitor; R_{CL}, the resistance to charge current; C_{ESC}, capacity of the energy storage capacitor; U_m, value of the maximum doubled voltage; C_{CL}, capacitance of the charging capacitor; GPED, gravitational press-electrode device

* Corresponding author.
E-mail address: agolberg@tauex.tau.ac.il (A. Golberg).

https://doi.org/10.1016/j.ifset.2020.102288
Received 23 February 2019; Received in revised form 6 January 2020; Accepted 6 January 2020
Available online 08 January 2020

Although the exact mechanism of the biological tissue permeabilization with PEF is not fully understood, PEF technology is currently used in multiple applications in medicine and biotechnology (Kotnik et al., 2015; Yarmush, Golberg, Serša, Kotnik, & Miklavčič, 2014). The current theory suggests that the membrane permeabilization is achieved through the formation of aqueous pores on the cell membrane, a phenomenon known as electroporation (Kotnik, Kramar, Pucihar, Miklavčič, & Tarek, 2012). In the food industry, PEF technology and processes recently gained momentum that resulted in several industrial-scale implementations (Sack et al., 2010; Sack, Schultheiss, & Bluhm, 2005) such as potato (Boussetta, Grimi, Lebovka, & Vorobiev, 2013; Hossain, Aguiló-Aguayo, Lyng, Brunton, & Rai, 2015; Lebovka, Shynkaryk, & Vorobiev, 2007), tomato (Luengo, Álvarez, & Raso, 2014), sugar beets (Jemai & Vorobiev, 2006; Loginova, Lebovka, & Vorobiev, 2011; Ma & Wang, 2013) and grape (Cholet et al., 2014; Medina-Meza & Barbosa-Cánovas, 2015) processing.

Nevertheless, unique physical characteristics of each plant biomass, the dynamics, and nature of its changes in electroporation require a case by case optimization of PEF parameters such as applied voltage, a number of pulses, pulse duration, frequency and temperature (Golberg et al., 2016). At the laboratory scale, several designs of pulse generators have been previously proposed (Hofmann, 2000; Novickij, Grainys, Novickij, Tolvaisiene, & Markovskaja, 2014; Pirc, Reberšek, & Miklavčič, 2017; Puc et al., 2004; Reberšek, Miklavcic, Bertacchini, & Sack, 2014; Reberšek, Miklavčič, & Miklavčič, 2010; Sack, Hochberg, & Mueller, 2016; Sack, Ruf, Hochberg, Herzog, & Mueller, 2017; Stankevič et al., 2013). However, most of them provide limited flexibility for coupled control of electrical and mechanical parameters that are necessary for designing processes that will enable upscaling of biomass processing (Reberšek et al., 2014; Bae, Kwasinski, Flynn, & Hebner, 2010).

The goal of this work was to develop a laboratory device with adaptive electrical and mechanical components to allow electroporation of the marine macroalgae biomass, an emerging feedstock for biorefinery (Buschmann et al., 2017; Fernand et al., 2016; Jiang, Ingle, & Golberg, 2016; Jung, Lim, Kim, & Park, 2013; Robin, Chavel, Chemodanov, Israel, & Golberg, 2017). Indeed, macroalgae fractionation with pulsed electric fields, once available, could lead to non-thermal, chemical-free extraction of valuable phytochemicals from cells such as proteins, amino acids, and carbohydrates (Polikovsky et al., 2016; Postma et al., 2017; Robin et al., 2018; Robin & Golberg, 2016). Recent studies proposed the use of PEF technologies also for the extraction of high-value compounds, including carotenoids, from algal biomass (Barba, 2017; Barba, Grimi, & Vorobiev, 2014; Poojary et al., 2016). Nevertheless, the use of currently available PEF technologies on seaweeds very limited because of their high salt content and, thus, high conductivity of the media (Barba et al., 2014). This leads to high currents in electric fields that are required for cell membrane permeabilization (Postma et al., 2017; Robin & Golberg, 2016). Furthermore, as the electrical conductivity of the biomass after electroporation increases (Polikovsky et al., 2016) and leads to an increase in pulse current and unacceptable heating of electroporated biomass, or heating beyond the energy dissipation capabilities of the device.

To address these challenges, we developed an adaptive pulsed electric field generator with a new circuit topology that allows controlling the voltage on each pulse in sequence. This control was achieved by a new topology with the asymmetric configuration of charging and discharging capacitors, where the large discharging capacitor is charged by small discrete charges supplied by a smaller additional capacitor. In addition, we developed a sliding press-electrode device for liquid-solid separation of macroalgae biomass during electroporation. The application of this electromechanical system was demonstrated on the electroporation of green macroalgae from *Ulva* sp., an emerging feedstock for marine biorefineries (Bikker et al., 2016; Chemodanov et al., 2017; Glasson, Sims, Carnachan, de Nys, & Magnusson, 2017). To monitor the electroporation progress, we used multifrequency electrical impedance spectroscopy (Castellví, Mercadal, & Ivorra, 2017; Ivorra, Villemejane, & Mir, 2010), which was reported in previous works as a cost-effective method for electroporation detection (Castellví et al., 2017; Golberg et al., 2016; Golberg, Laufer, Rabinowitch, & Rubinsky, 2011).

2. Materials and methods

2.1. Macroalgae Ulva sp. biomass

Ulva sp., taken from stocks cultivated in an outdoor seaweed collection at Israel Oceanographic & Limnological Research, Haifa, Israel (IOLR), was grown under controlled conditions in using 40 L macroalgae photobioreactors (MPBR) incorporated in a building's south wall under daylight conditions in a system described in ref. (Chemodanov, Robin, & Golberg, 2017). Nutrients were supplied by adding ammonium nitrate (NH_4NO_3) and phosphoric acid (H_3PO_4), (Haifa Chemicals Ltd., IS) to maintain 6.4 g m^{-3} of total nitrogen and 0.97 g m^{-3} of total phosphorus in the seawater. The sole CO_2 source was bubbled air. Other conditions such as pH (8.2), salinity, and airflow rate (2–4 L min^{-1}) were maintained steady in all the reactors. The surface water was removed from the harvested biomass with a standard protocol by centrifuging the algal biomass in an electric centrifuge (Beswin Portable Washer Spin Dryer CE-88 (6.0 kg) 2800RPM Stainless Steel Housing) until all surface water was removed (< 1 mL separated).

2.2. Ulva sp. biomass electroporation

Ulva sp. biomass was harvested and centrifuged in a manual kitchen centrifuge to remove the surface water 3 times for 2 min. For PEF treatment, 1 g of the fresh weight (FW) biomass was loaded in the electroporation chamber and PEF was applied. The used protocol was 124 ± 12 V mm^{-1}, pulse duration 50 μs, pulse number 50, frequency 3 Hz. Currents on the cell were registered in real-time with a PicoScope 4224 Oscilloscope with a Pico Current Clamp (60A AC/DC) and analyzed with Pico Scope 6 software (Pico technologies Inc., UK). The extracted and separation liquid fraction was collected at the bottom of the device. The experiment was repeated three times.

2.3. Impedance measurement and data analysis

The impedance of the sample, within the electroporation chamber, were measured with a Vector Network Analyzer (Keysight Inc. USA model E5061B). The accuracy of the measurement was validated by measuring standard 10 Ω and 100 Ω resistors in parallel with a 1 μF capacitor, with marginal parasitic resistance and capacitance verified. Measurements were performed in the frequency range from 5 Hz to 1 MHz in 1600 steps logarithmically spaced. Both magnitude and phase data were recorded in a Bode export setting. A non-parametric statistical U-Mann Whitney test was used to compare data from treated samples and data from control samples at each frequency. Statistically significant differences were considered for p-value < 0.05.

The experimental impedance data from 2 kHz to 1 MHz was later heuristically fitted to a mathematical model. The model used to fit the experimental data consists in a Constant Phase Element (CPE), to model the impedance behavior of the electrode-electrolyte interface, in series with a Cole impedance equation to model the impedance behavior of sample (Grimnes & Martinsen, 2008):

$$Z(\omega) = Z_{CPE}(\omega) + Z_{Cole}(\omega) = \left(\frac{1}{Q_0(j\omega)^n}\right) + \left(R_\infty + \frac{R_0 - R_\infty}{1 + (j\omega\tau)^\alpha}\right) \quad (1)$$

where ω is the angular frequency (in rads/s) and j is the unit imaginary number. In the Cole equation ($Z_{Cole}(\omega)$), R_∞ would correspond to the sample impedance at an infinite frequency, R_0 would correspond to the sample impedance at zero frequency, τ would be the characteristic time

constant of the sample and α is a dimensionless parameter with a theoretical value between 0 and 1; in practice between 0.5 and 1. This equation results from modeling the cellular system as an electrical circuit consisting of resistance, representing the extracellular medium, combined in parallel with the series combination of another resistance, representing the intracellular medium, and a capacitance representing the cell membrane. The equation employed to model the impedance behavior of the electrode-electrolyte interface ($Z_{CPE}(\omega)$) is commonly used to model the behavior of an imperfect capacitor. Q_0 is the capacitance and n is a dimensionless parameter that, similarly to the case of the α parameter, can have a theoretical value between 0 and 1 but, in practice, it lies between 0.5 and 1. Note that if $n = 1$ this equation would be equivalent to an ideal capacitor.

The cell disintegration index (Bobinaitė et al., 2014; Donsì, Ferrari, Fruilo, & Pataro, 2010) (Z_p) was calculated on the basis of the measurement of the absolute impedance value of control (Z_c) and PEF-treated tissue (Z_{tr}) in the low (1 kHz) and high (1 MHz) frequency ranges accordingly with (Bobinaitė et al., 2014; Donsì et al., 2010), as follows:

$$Z_p = \frac{|Z_{c(1\ kHz)}| - |Z_{tr(1\ kHz)}|}{|Z_{c(1\ kHz)}| - |Z_{tr(1MHz)}|} \quad (2)$$

where the value of Z_p varies between 0 for intact tissue and 1 for fully permeabilized tissue.

3. Results and discussion

3.1. High-voltage pulse generator with asymmetric voltage doubler topology

The schematic representation of the key elements of the developed high-voltage pulse generator is shown in Fig. 1a. The generator provides the following specifications: 4000 V (max), 1.5 kA (max), 1–100 μs pulse duration. The system consists of

1) charging device: zero voltage switch power controller and zero voltage power switch for connection of the network and High Voltage Transformer that supply charge to capacitors (ESC); voltage doubler with a small charging capacitor (to enable step charging of the energy storage capacitor, enabling applied voltage control of each pulse);
2) ESC: Capacitor, discharging resistor (for safety and charge control for each pulse) and high voltage switch (for pulse shape control).
3) electroporation cell (EPC): chamber with electrodes applied to the biomass and.
4) microcontroller, which regulates the parameters for each pulse.

The main functional elements of the electronic system (Fig. 1b) are: two parallel-connected ESC with a total capacity of 100 μF with a voltage rating of 6 kV (Maxwell, CA, USA, cat#34083, custom made); a high-voltage source to charge of energy storage capacitors; circuit node for the discharge of ESC; a high-voltage switch for the pulsed discharge of ESC on treated biomass (Fast High Voltage Transistor Switch HTS 61-240-SI for voltage 6 kV and current 2.4 kA (BEHLKE, Germany); circuit node for manual control of high-voltage contactor in testing mode; microcontroller. Importantly, there is no possibility of an active current limitation in the switch. Therefore, a series connection of a low-inductance resistor, calculated for the maximum impulse current, is necessary to provide for passive current-limitation during the discharge. A current limiting resistor with 2.5 Ω was chosen (FPA250, 2.5 Ω, 250 W, ARCOL, UK).

The high-voltage source for charging the energy storage capacitors consists of a step-up transformer of 220/2000 V, a voltage doubler, and an ESC voltage-regulating unit. The voltage doubler (Fig. 1b) consists of two high-voltage diodes and two capacitors of dissimilar capacitance. That is, the architecture of the voltage doubler is asymmetric. To the best of our knowledge, this is a new feature. The first capacitor acts as a charging capacitor that, in addition to the voltage doubling function, performs the function of current limitation when the ESC is charged. The second capacitor is the ESC. The choice of the capacity of the charging capacitor is determined by requirements that are related to the current limitation function for ESC charging, the necessary power of the electroporation process and the acceptable accuracy of the electroporation voltage setting.

The process of ESC charge using an asymmetric voltage doubler occurs according to the exponential law (Fig. 1c).

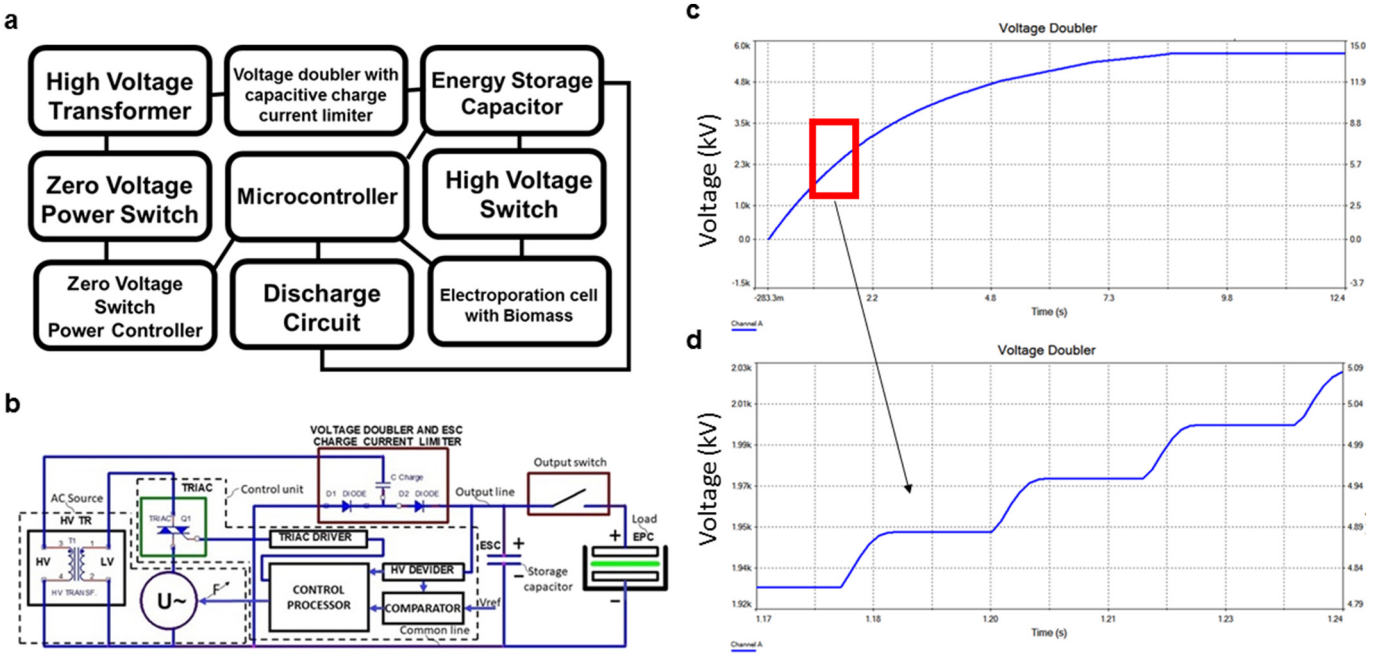

Fig. 1. a. Conceptual scheme of the laboratory pulsed electric field based system for biomass electroporation. b. Main components of the pulse generator. c–d. ESC charging process c. low magnification. d. High magnification shows the principle of small step (quantum) charging provided by the asymmetric design of the voltage doubler.

$$U_{ESC} = 1 - U_m e^{\frac{-t}{R_{CL} C_{ESC}}} \quad (3)$$

U_{ESC} is the voltage on the storage capacitor, R_{CL} is the resistance to charge current, and C_{ESC} - the capacity of the energy storage capacitor (100 μF); U_m - the value of the maximum doubled voltage (5657 V), *t* is time.

An increase in the voltage on the ESC occurs at each cycle of the sinusoidal voltage when the charging capacitor is recharged. The process of ESC charge has a discrete and portioning character, which is depicted in Fig. 1d, enable voltage control for each pulse. A discrete voltage increment occurs on the ESC every cycle. The magnitude of this increment depends on the difference between the accumulated and maximum voltage. The value of the discrete voltage increments (dU) in the process of ESC charge is described as the inversely proportional function:

$$dU = \frac{C_{CL} U_m}{C_{ESC}} \bullet \left(1 - \frac{U_{ESC}}{U_m}\right) \quad (4)$$

where C_{CL} is the capacitance of the charge capacitor (0.7 μF); U - the value of the voltage on the ESC (600–4000 V). For example, a discrete increment of voltage on the ESC for one period at an existing voltage U_{ESC} = 0 V will be dU = 39.6 V. With the accumulated voltage U_{ESC} = 1000 V, the voltage on the ESC will be equal to dU = 32.6 V. At U_{ESC} = 2000 V, dU = 25.6 V. At a voltage U_{ESC} = 3000 V, dU = 18.6 V and at U_{ESC} = 4000 V, dU = 11.6 V. Thus, within a range of voltages required for electroporation, the charge source can theoretically provide the accuracy of the voltage setting from 5 to 0.4%, depending on the voltage value on the ESC. The voltage required for the electroporation on the ESC is set by the method of discrete control of charge by means of an electrical circuit of comparing the set and actual voltage.

3.2. Gravitational press-electrode device for biomass electroporation

The main elements of the mechanical part of the developed laboratory device are EPC (Fig. 2a), EPC holder (Fig. 2a), the contact assembly of the EPC, the gravity press-electrode device and a high-voltage blocker (Fig. 2b). The EPC is designed to hold the biomass in the space between the electrodes during electroporation. EPC also allows continuous separation biomass into liquid and cake simultaneously with the application of PEF.

The EPC (Fig. 2a) consists of three parts: a plastic body (Teflon) of a cylindrical shape (2.5 cm diameter), the positive electrode (stainless steel), located at the lower part of the cylinder and the plug-type contact for the connection with power supply. In the lateral part of the EPC body, there are narrow slit-like openings (1 by 5 mm) for the outlet of the liquid fraction that is extracted by PEF (Fig. 2a). The extracted liquid is collected through a groove at the base of the EPC.

The gravitational press-electrode device (GPED, 1604 g) with sliding electrodes, is shown in Fig. 2b.

The device separates the electroporated biomass into liquid and solid fractions. Up to 10 kg load can be applied to pressurize the biomass during and after pulsed electric field treatment (Fig. 2b). A displacement sensor (optoNCDT, Micro-Epsilon, NC), is installed on the GPED to monitor the volume change of the biomass. The shapes of voltage and current on seaweed inside the GPED device are shown in Fig. 2c.

3.3. Green macroalgae Ulva sp. electroporation

During the application of the PEF, the current increased from 11 ± 2 A at the first pulse to 33 ± 6 A at the last pulse. The volume change of the biomass, due to both juice extraction and compaction because of electroporation was 1.39 ± 0.29 cm^3 (the original volume of the biomass was 13.7 ± 3.5 cm^3). The volume change suggested the electroporation of the *Ulva* sp., cells, and extraction of the intracellular content. Previous studies on extraction of organic compounds from microalgae showed that modification of the pH (Parniakov et al., 2015a) and use of binary mixtures of solvents, for example, DMSO or ethanol and water (Parniakov et al., 2015b) significantly improved the yields and purity of the extracted compounds. Future work with macroalgae should incorporate these findings if the extraction of organic compounds is needed.

Impedance spectrum changes were observed in the PEF treated Ulva biomass in relation to non-treated biomass (Fig. 3). Statistically

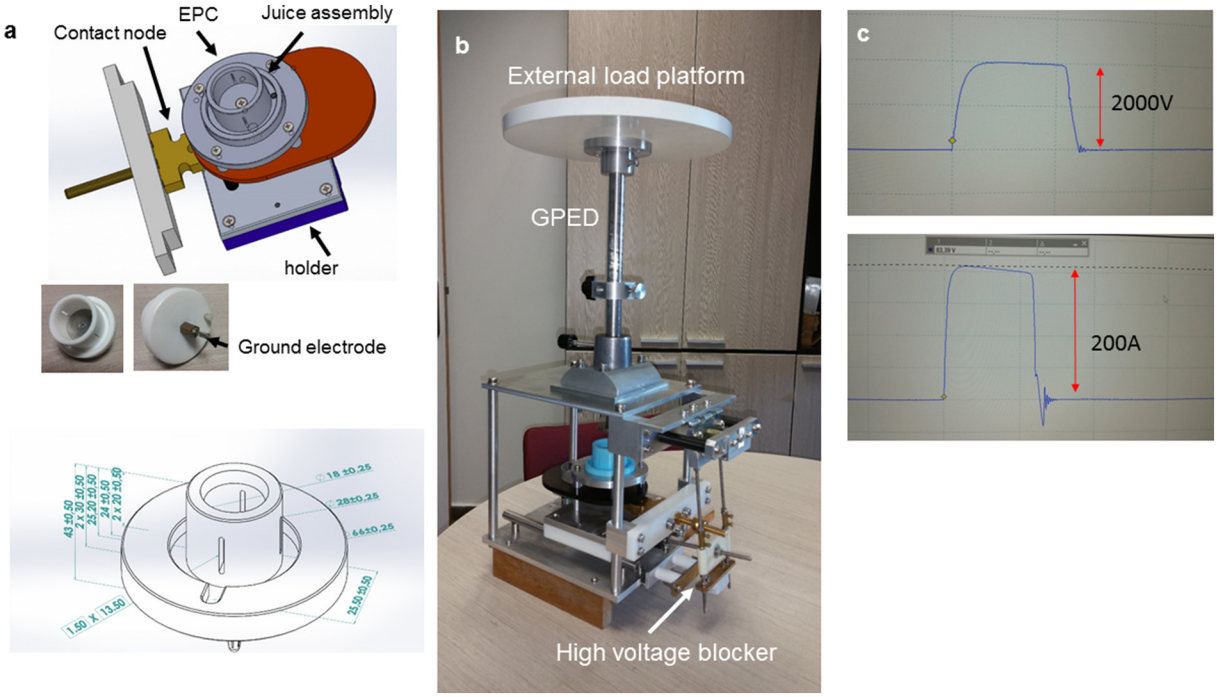

Fig. 2. a. Electroporation cell. The top figure shows the design of the EPC module. Bottom digital images show the final EPC with contact electrodes. b. The gravitational press-electrode device. c. Voltage and current shapes during pulse application.

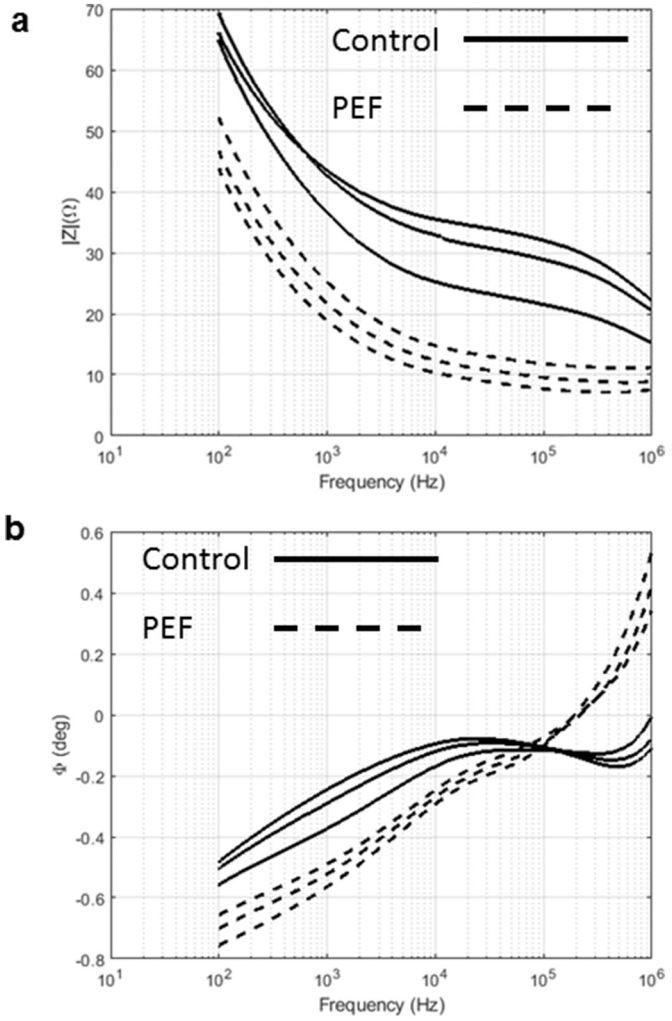

Fig. 3. Magnitude (a) and phase (b) bioimpedance spectra of PEF treated samples (dashed lines) and untreated control samples (solid lines) conditions. Significance statistical differences are observed above 0.1 kHz and 0.1 to 1 kHz for magnitude and phase respectively ($P < 0.05$). n = 3 all data points are shown.

significant differences (p-value < 0.05) were observed in the whole frequency range above 0.1 kHz as well as in the range of 0.1 to 1 kHz for magnitude (Fig. 3a) and phase (Fig. 3b) parameters respectively. The bioimpedance changes are associated in general with a modification of the volumetric resistance and reactance of the biomass samples. The untreated biomass displayed the common features of a so-called β dispersion in the frequency range from about 10 kHz to 1 MHz. At lower frequencies (< 10 kHz) the impedance of the electrode-electrolyte interface dominates. The occurrence of a β dispersion is more obviously manifested in Fig. 4 where the presence of a semicircle is observed in the imaginary part versus the real part plot of the impedance. Such behavior is indicative of a dense assembly of living cells. In that figure the electrode-electrolyte interface produces a straight line of about 45 degrees. In the treated samples the β dispersion disappeared. In those cases, the behavior is equivalent to that of two electrodes in a saline medium. This indicates that the cell membranes, which are responsible for the β dispersion because of their dielectric nature, were destroyed or severely permeated (Ivorra, 2010). The average value of the disintegration index was 0.63.

The parameters obtained by fitting the data to the mathematical model (Eq. (1)) are indicated in Table 1. In the PEF treated samples, the cell membrane is short-circuited and therefore the model becomes a CPE in series with an ideal resistor (represented as R_0 in the table).

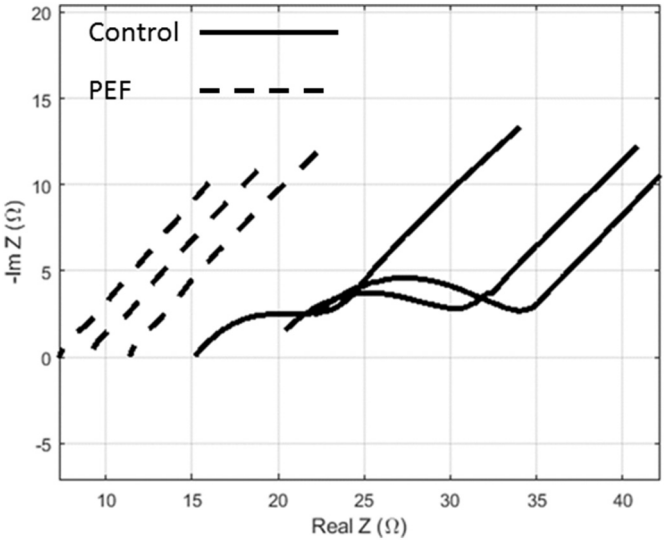

Fig. 4. Imaginary part versus the real part of the impedance for PEF treated samples (dashed lines) and untreated control samples (solid lines). The impedance of untreated samples is represented between 1 kHz and 1 MHz. The impedance of treated samples is represented only up to 200 kHz to avoid representing the distortion that occurs at high frequencies due to the presence of parasitic inductances. n = 3 all data points are shown.

Since R_∞ is determined by the parallel association of the intracellular and extracellular resistances, a similar value would be expected for the resistance in the PEF treated samples if we only consider this short-circuiting effect. However, the values obtained are significantly lower than the R_∞ values in the control samples. Thus, the results cannot be explained simply by the increase in the conduction through the membrane. To explain these results, it is necessary to take into account the ionic release from the cells to the extracellular medium. This release causes a large increase in the extracellular medium conductivity, which is initially very low compared to the intracellular conductivity. Thus, due to the ion release, the extracellular resistance is significantly reduced and values lower than R_∞ are measured after PEF treatment.

4. Conclusions

New methods and devices are needed for PEF technology optimization for highly conductive marine macroalgae biomass. In this work, we report the architecture of a PEF system, which consists of a pulsed electric field generator with an asymmetric voltage multiplier and a treatment chamber with sliding electrodes. The developed system allows applying pulses of up to 4 kV and 1 kA with a pulse duration between 1 μs and 100 μs, and up to 10 kg of mechanical load. The combination of the pulse generator with the sliding electrodes provides continuous liquid phase extraction during electroporation. Furthermore, bioimpedance can be used to monitor seaweed biomass electroporation. The system was demonstrated on the electroporation of green marine macroalgae from *Ulva* sp., an emerging biorefinery feedstock.

Declaration of authors' contributions

KL designed and build the electroporation system, KL, YL, AG conducted the experiments and measurements, BM, AI, and CAG analyzed the impedance data, KL, AI, CAG and AG drafted the manuscript. AG conceived the study. All authors read and approved the manuscript.

Declaration of competing interest

None.

Table 1
Values of the parameters obtained by fitting the impedance data to the model of Eq. (1) – stays for parameters that were not possible to fit in this model.

	Control				PEF treated samples			
	1	2	3	Average ± SD	1	2	3	Average ± SD
R_0 (Ω)	29.5	22.5	33.4	28 ± 5.5	11.2	9.3	8.0	9.5 ± 1.6
R_∞ (Ω)	19	14.5	21.1	18 ± 3	–	–	–	–
τ (s)	$4.60{\cdot}10^{-7}$	$4.50{\cdot}10^{-7}$	$4.70{\cdot}10^{-7}$	$(4.6 \pm 0.1){\cdot}10^{-7}$	–	–	–	–
α	0.75	0.63	0.78	0.72 ± 0.08	–	–	–	–
$Q_0(\Omega^{-1})$	$5.00{\cdot}10^{-4}$	$3.90{\cdot}10^{-4}$	$4.50{\cdot}10^{-4}$	$(4.5 \pm 0.6){\cdot}10^{-4}$	$5.4{\cdot}10^{-4}$	$5.8{\cdot}10^{-4}$	$5.5{\cdot}10^{-4}$	$(5.6 \pm 0.2){\cdot}10^{-4}$
n	0.55	0.565	0.58	0.57 ± 0.02	0.54	0.54	0.56	0.55 ± 0.01

CRediT authorship contribution statement

Klimentiy Levkov: Conceptualization, Formal analysis, Investigation, Methodology, Writing - original draft. **Yoav Linzon:** Formal analysis, Investigation, Methodology. **Borja Mercadal:** Formal analysis, Investigation, Methodology. **Antoni Ivorra:** Formal analysis, Writing - review & editing. **César Antonio González:** Formal analysis, Investigation, Methodology, Writing - review & editing. **Alexander Golberg:** Conceptualization, Formal analysis, Investigation, Methodology, Writing - original draft, Funding acquisition.

Acknowledgments

The authors thank the Israel Ministry of Science and Technology for the support of this work.

Statement of informed consent, human/animal rights

No conflicts, informed consent, human or animal rights applicable.

References

Bae, S., Kwasinski, A., Flynn, M. M., & Hebner, R. E. (2010). High-power pulse generator with flexible output pattern. *IEEE Transactions on Power Electronics, 25*(7), 1675–1684.

Barba, F. J. (2017). Microalgae and seaweeds for food applications: Challenges and perspectives. *Food Research International,* 969–970.

Barba, F. J., Grimi, N., & Vorobiev, E. (2014). New approaches for the use of non-conventional cell disruption technologies to extract potential food additives and nutraceuticals from microalgae. *Food Engineering Reviews, 7*(1), 45–62.

Bikker, P., Krimpen, M. M., Wikselaar, P., Houweling-Tan, B., Scaccia, N., Hal, J. W., ... Cone johncone, J. W. (2016). Biorefinery of the green seaweed Ulva lactuca to produce animal feed, chemicals and biofuels. *Journal of Applied Phycology, 28*, 3511–3525.

Bobinaitė, R., Pataro, G., Lamanauskas, N., Šatkauskas, S., Viškelis, P., & Ferrari, G. (2014). Application of pulsed electric field in the production of juice and extraction of bioactive compounds from blueberry fruits and their by-products. *Journal of Food Science and Technology, 52*(9), 5898–5905.

Boussetta, N., Grimi, N., Lebovka, N. I., & Vorobiev, E. (2013). "Cold" electroporation in potato tissue induced by pulsed electric field. *Journal of Food Engineering, 115*(2), 232–236.

Bugge, M. M., Hansen, T., & Klitkou, A. (2016). What is the bioeconomy? A review of the literature. *Sustainability, 8*(7), 691.

Buschmann, A. H., Camus, C., Infante, J., Neori, A., Israel, Á., Hernández-González, M. C., ... Critchley, A. T. (2017). Seaweed production: Overview of the global state of exploitation, farming and emerging research activity. *European Journal of Phycology, 52*(4), 391–406.

Castellví, Q., Mercadal, B., & Ivorra, A. (2017). Assessment of electroporation by electrical impedance methods. *Handbook of electroporation*https://doi.org/10.1007/978-3-319-32886-7_164.

Chemodanov, A., Jinjikhashvily, G., Habiby, O., Liberzon, A., Israel, A., Yakhini, Z., & Golberg, A. (2017). Net primary productivity, biofuel production and CO2 emissions reduction potential of Ulva sp. (Chlorophyta) biomass in a coastal area of the Eastern Mediterranean. *Energy Conversion and Management, 148*, 1497–1507.

Chemodanov, A., Robin, A., & Golberg, A. (2017). Design of marine macroalgae photobioreactor integrated into building to support seagriculture for biorefinery and bioeconomy. *Bioresource Technology, 241*, 1084–1093.

Cholet, C., Delsart, C., Petrel, M., Gontier, E., Grimi, N., L'Hyvernay, A., ... Geny, L. (2014). Structural and biochemical changes induced by pulsed electric field treatments on cabernet sauvignon grape berry skins: Impact on cell wall total tannins and polysaccharides. *Journal of Agricultural and Food Chemistry, 62*(13), 2925–2934.

Donsì, F., Ferrari, G., Fruilo, M., & Pataro, G. (2010). Pulsed electric field-assisted vinification of aglianico and piedirosso grapes. *Journal of Agricultural and Food Chemistry, 58*(22), 11606–11615.

Fernand, F., Israel, A., Skjermo, J., Wichard, T., Timmermans, K. R., & Golberg, A. (2016). Offshore macroalgae biomass for bioenergy production: Environmental aspects, technological achievements and challenges. *Renewable and Sustainable Energy Reviews, 75*(October), 35–45.

Glasson, C. R. K., Sims, I. M., Carnachan, S. M., de Nys, R., & Magnusson, M. (2017). A cascading biorefinery process targeting sulfated polysaccharides (ulvan) from Ulva ohnoi. *Algal Research, 27*, 383–391.

Golberg, A., Laufer, S., Rabinowitch, H. D., & Rubinsky, B. (2011). In vivo non-thermal irreversible electroporation impact on rat liver galvanic apparent internal resistance. *Physics in Medicine and Biology, 56*(4), 951–963.

Golberg, A., Sack, M., Teissie, J., Pataro, G., Pliquett, U., Saulis, G., ... Frey, W. (2016). Energy efficient biomass processing with pulsed electric fields for bioeconomy and sustainable development. *Biotechnol. Biofuels, 9*(1), 1.

Grimnes, S., & Martinsen, Ø. (2008). Bioimpedance and bioelectricity basics. *Bioimpedance and bioelectricity basics*.

Günerken, E., D'Hondt, E., Eppink, M. H. M., Garcia-Gonzalez, L., Elst, K., & Wijffels, R. H. (2015). Cell disruption for microalgae biorefineries. *Biotechnology Advances, 33*(2), 243–260.

Hofmann, G. A. (2000). Instrumentation and electrodes for in vivo electroporation. *Electrochemotherapy, electrogenetherapy, and transdermal drug delivery* (pp. 37–61). New Jersey: Humana Press.

Hossain, M. B., Aguiló-Aguayo, I., Lyng, J. G., Brunton, N. P., & Rai, D. K. (2015). Effect of pulsed electric field and pulsed light pre-treatment on the extraction of steroidal alkaloids from potato peels. *Innovative Food Science and Emerging Technologies, 29*, 9–14.

Ivorra, A. (2010). *Tissue electroporation as a bioelectric phenomenon: Basic concepts.* Berlin, Heidelberg: Springer23–61.

Ivorra, A., Villemejane, J., & Mir, L. M. (2010). Electrical modeling of the influence of medium conductivity on electroporation. *Physical Chemistry Chemical Physics, 12*(34), 10055–10064.

Jemai, A. B., & Vorobiev, E. (2006). Pulsed electric field assisted pressing of sugar beet slices: Towards a novel process of cold juice extraction. *Biosystems Engineering, 93*(1), 57–68.

Jiang, R., Ingle, K. N., & Golberg, A. (2016). Macroalgae (seaweed) for liquid transportation biofuel production: What is next? *Algal Research, 14*, 48–57.

Jung, K. A., Lim, S.-R. R., Kim, Y., & Park, J. M. M. (2013). Potentials of macroalgae as feedstocks for biorefinery. *Bioresource Technology, 135*, 182–190.

Kotnik, T., Kramar, P., Pucihar, G., Miklavčič, D., & Tarek, M. (2012). Cell membrane electroporation - Part 1: The phenomenon. *IEEE Electrical Insulation Magazine, 28*(5), 14–23.

Kotnik, T., Frey, W., Sack, M., Haberl Meglič, S., Peterka, M., & Miklavčič, D. (2015). Electroporation-based applications in biotechnology. *Trends in Biotechnology, 33*(8), 480–488.

Lebovka, N. I., Shynkaryk, N. V., & Vorobiev, E. (2007). Pulsed electric field enhanced drying of potato tissue. *Journal of Food Engineering, 78*(2), 606–613.

Lee, S. Y., Cho, J. M., Chang, Y. K., & Oh, Y. K. (2017). Cell disruption and lipid extraction for microalgal biorefineries: A review. *Bioresource Technology, 244*, 1317–1328 2.

Loginova, K. V., Lebovka, N. I., & Vorobiev, E. (2011). Pulsed electric field assisted aqueous extraction of colorants from red beet. *Journal of Food Engineering, 106*(2), 127–133.

Luengo, E., Álvarez, I., & Raso, J. (2014). Improving carotenoid extraction from tomato waste by pulsed electric fields. *Frontiers in Nutrition, 1*, 12.

Ma, S., & Wang, Z. H. (2013). Pulsed electric field-assisted modification of pectin from sugar beet pulp. *Carbohydrate Polymers, 92*(2), 1700–1704.

Maity, S. K. (2015). Opportunities, recent trends and challenges of integrated biorefinery: Part II. *Renewable and Sustainable Energy Reviews, 43*, 1446–1466.

Medina-Meza, I. G., & Barbosa-Cánovas, G. V. (2015). Assisted extraction of bioactive compounds from plum and grape peels by ultrasonics and pulsed electric fields. *Journal of Food Engineering, 166*, 268–275.

Mussatto, S. I. (2016). *Biomass fractionation technologies for a lignocellulosic feedstock based biorefinery. Biomass fractionation technologies for a lignocellulosic feedstock based biorefinery*.

Novickij, V., Grainys, A., Novickij, J., Tolvaisiene, S., & Markovskaja, S. (2014). Compact electro-permeabilization system for controlled treatment of biological cells and cell medium conductivity change measurement. *Meas. Sci. Rev. 14*(5), 279–284.

Parniakov, O., Barba, F. J., Grimi, N., Marchal, L., Jubeau, S., Lebovka, N., & Vorobiev, E. (2015a). Pulsed electric field and pH assisted selective extraction of intracellular components from microalgae nannochloropsis. *Algal Research, 8*, 128–134.

Parniakov, O., Barba, F. J., Grimi, N., Marchal, L., Jubeau, S., Lebovka, N., & Vorobiev, E.

(2015b). Pulsed electric field assisted extraction of nutritionally valuable compounds from microalgae Nannochloropsis spp. using the binary mixture of organic solvents and water. *Innovative Food Science and Emerging Technologies, 27*, 79–85.
Pirc, E., Reberšek, M., & Miklavčič, D. (2017). Dosimetry in electroporation-based technologies and treatments. *Dosimetry in bioelectromagnetic* (pp. 233–268). Boca Raton: CRC Press.
Polikovsky, M., Fernand, F., Sack, M., Frey, W., Müller, G., & Golberg, A. (2016). Towards marine biorefineries: Selective proteins extractions from marine macroalgae Ulva with pulsed electric fields. *Innovative Food Science & Emerging Technologies, 37*, 194–200.
Poojary, M. M., Barba, F. J., Aliakbarian, B., Donsì, F., Pataro, G., Dias, D. A., & Juliano, P. (2016). Innovative alternative technologies to extract carotenoids from microalgae and seaweeds. *Marine Drugs, 14*(11) pii: E214.
Postma, P. R., Cerezo-Chinarro, O., Akkerman, R. J., Olivieri, G., Wijffels, R. H., Brandenburg, W. A., & Eppink, M. H. M. (2017). Biorefinery of the macroalgae Ulva lactuca: Extraction of proteins and carbohydrates by mild disintegration. *Journal of Applied Phycology*, 1–13.
Puc, M., Čorović, S., Flisar, K., Petkovšek, M., Nastran, J., & Miklavčič, D. (2004). Techniques of signal generation required for electropermeabilization. Survey of electropermeabilization devices. *Bioelectrochemistry, 64*(2), 113–124.
Reberšek, M., Miklavcic, D., Bertacchini, C., & Sack, M. (2014). Cell membrane electroporation-Part 3: The equipment. *IEEE Electrical Insulation Magazine, 30*(3), 8–18.
Reberšek, M., Miklavčič, D., & Miklavčič, D. (2010). *Concepts of electroporation pulse generation and overview of electric pulse generators for cell and tissue electroporation.* 343–360.
Rinaldi, R. (2014). Plant biomass fractionation meets catalysis. *Angew. Chem. Int. Ed., 53*(33), 8559–8560.
Robin, A., Chavel, P., Chemodanov, A., Israel, A., & Golberg, A. (2017). Diversity of monosaccharides in marine macroalgae from the Eastern Mediterranean Sea. *Algal Research, 28*, 118–127.
Robin, A., & Golberg, A. (2016). *Pulsed electric fields and electroporation technologies in marine macroalgae biorefineries.* 1–16.
Robin, A., Kazir, M., Sack, M., Israel, A., Frey, W., Mueller, G., & Golberg, A. (2018). Functional protein concentrates extracted from the green marine macroalga *Ulva* sp., by high voltage pulsed electric fields and mechanical press. *ACS Sustainable Chemistry & Engineering, 6*(11), 13696–13705.
Sack, M., Hochberg, M., & Mueller, G. (2016). Synchronized switching and active clamping of IGBT switches in a simple marx generator. *PCIM Europe 2016; International exhibition and conference for power electronics, intelligent motion, renewable energy and energy management*.
Sack, M., Sigler, J., Frenzel, S., Eing, C., Arnold, J., Michelberger, T., ... Müller, G. (2010). Research on industrial-scale electroporation devices fostering the extraction of substances from biological tissue. *Food Engineering Reviews, 2*(2), 147–156.
Sack, M., Ruf, J., Hochberg, M., Herzog, D., & Mueller, G. (2017). A device for combined thermal and pulsed electric field treatment of food. *2017 international conference on optimization of electrical and electronic equipment (OPTIM) & 2017 intl aegean conference on electrical machines and power electronics (ACEMP)* (pp. 31–36). IEEE.
Sack, M., Schultheiss, C., & Bluhm, H. (2005). Triggered Marx generators for the industrial-scale electroporation of sugar beets. *IEEE Transactions on Industry Applications, 41*(3), 707–714.
Stankevič, V., Novickij, V., Balevičius, S., Žurauskiene, N., Baškys, A., Dervinis, A., & Bleizgys, V. (2013). Electroporation system generating wide range square-wave pulses for biological applications. *2013 IEEE biomedical circuits and systems conference, BioCAS 2013*.
Yarmush, M. L., Golberg, A., Serša, G., Kotnik, T., & Miklavčič, D. (2014). Electroporation-based technologies for medicine: Principles, applications, and challenges. *Annual Review of Biomedical Engineering, 16*, 295–320.